Short communication

Novel proton conducting polymer electrolytes based on polyparabanic acid doped with H_3PO_4 for high temperature fuel cell

Yuichi Aihara*, Atsuo Sonai

Samsung Yokohama Research Institute, 2-7 Sugasawa-cho, Tsurumi, Yokohama 230-0027, Japan

Abstract

Three novel proton conducting polymer electrolytes based on polyparabanic acid doped with H_3PO_4 were synthesized and their use in high temperature fuel cells characterized. The precursor polymers, PMD-Im, POD-Im and PDMDP-Im, were synthesized by cyclization polymerization of diisocynanates. After doping with H_3PO_4, the ionic conductivity and the thermal degradation were studied by using the AC impedance method and thermal gravimetric analysis, respectively. These membranes showed high ionic conductivity of the order of $10^{-2}\,S\,cm^{-1}$ at 423 K with good thermal stability. Their application to fuel cells was demonstrated and polarization curves were obtained at 423 K were obtained without humidification.
© 2006 Elsevier B.V. All rights reserved.

Keywords: Proton conduction; Fuel cell; Polymer electrolyte membrane; Polyparabanic acid

1. Introduction

Proton conductive polymer electrolytes have attracted attention since their applicability to polymer electrolyte membrane fuel cells (PEMFC) was suggested for stationary and/or transportation power generation. To enable the practical usage of PEMFC, further developments are still necessary, especially improvements in durability, applicability to a wider temperature range, and lower production costs. The high temperature PEMFC is a likely candidate for solving these difficulties and has received considerable attention over the last decade. Although there are some risks, e.g. isolation of catalyst and durability of organic compounds at high temperature, the long-life cell performance and good energy efficiency are expected due to the increase of catalytic activity at high temperature (with low carbon monoxide poisoning) and simpler water management. Also above 100 °C stable proton conducting media, such as phosphoric acid, is required instead of water.

Savinell and co-workers suggested the use of Brönsted acid doping polybenzimidazole for high temperature PEM-FCs [1–3]. Also, several proton conducting materials composed of various polymers and Brönsted acid (e.g. polyethyleneoxide–H_3PO_4 [4], polyvinylpyrolidone–H_3PO_4 [5], poly(acrylic acid)–NH_4HSO_4, polyethylene imine–H_2SO_4 [6], and Nylon–H_3PO_4 [7]) have been suggested for use in electrochemical devices including fuel cells since the 1980's. However, even if the proton conduction is acquired by doping with H_3PO_4, there may still be problems with the thermal stability of the polymers at high temperatures. Since the compatibility of thermal resistive plastics for acid doping polymer electrolytes is limited, few power generation tests were performed using polymer electrolytes at high temperature under low humidity conditions.

The polyparabanic acids (PPAs) were first used as an alternative to polyimide in 1971 [8]. Previously, Kanbara et al. found that large amounts of alkaline metal salts can be dissolved in PPAs, and high ionic conductivities obtained [9]. Also its thermal stability is attractive due to its high glass transition temperature (623 K). In the present study, the precursor polymers, PPAs were swelled in H_3PO_4 solutions to obtain the ionic conductivity. The temperature dependence of the ionic conductivity and the thermal stability of the polymer electrolytes were measured. Then the performance of the three electrolytes derived from the precursor polymers of PPA in high temperature fuel cells was investigated.

* Corresponding author. Tel.: +81 45 510 3971; fax: +81 45 510 3368.
  E-mail address: yuichi.aihara@samsung.com (Y. Aihara).

2. Experimental procedure

2.1. Synthesis and structure of precursor polymers of PPA

Three precursors of polyparabanic acid, PMD-Im **1**, POD-Im **2** and PDMDP-Im **3** were synthesized from hydrogen cyanide and 4,4′-diphenylmethane diisocyanate (TCI), 4,4′-diphenyl ether diisocyanate (Aldrich) and 3,3′-dimethoxy-4,4′-biphenylene diisocyanate (Aldrich), respectively, according to the patented method (Scheme 1) [8].

After purification by washing in methanol, the polymers were dried for 1 day at 60 °C under a vacuum of 0.1 Torr. The molecular weights were determined using GPC (Eluent: DMF, Columns: TOSOH α-M × 2, RI: Waters model 2414, polystyrene standard was used for a calibration). The polymer structures were determined from elemental analysis (JM10, J-Science), FT-IR (AVATAR 370, Nicole) and ^{1}H NMR (DMSO-d_6, 400 MHz, JNM LR400, JEOL).

2.2. Preparation of H₃PO₄ doped polymer electrolytes

To prepare the 10 wt.% polymer solution, the polymers were independently dissolved in *N*-methyl-2-pyrrolidone and stirred at room temperature for 24 h. After filtration, the polymer solutions were cast on a glass plate. The precursor polymer films were removed from the plate after evaporation of the solvent for 2 h at 333 K, and vacuum drying (0.1 Torr) for 18 h at 333 K. To obtain the proton conducting membrane, the precursor polymers were doped by immersion for 20 min in different concentrations (85%, and 93–99%) of phosphoric acid at 333 K. The doped polymers were put into an oven at 393 K to remove residual water and to form hydrolyzed PPA structures.

2.3. Thermal decomposition and ionic conductivity determination

Thermogravimetry (TG) was performed using a TG/DTA6200 (Seiko Instruments Inc.). The samples were put into an open platinum pan and scanned from 313 to 1173 K with a scanning rate of 10 K min^{-1}. The measurements were performed under Ar gas.
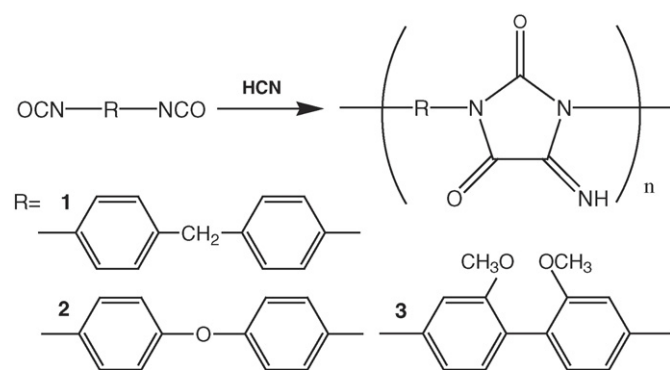
The ionic conductivities were determined using the AC impedance method on an Autolabo PGSTAT30 (Eco Chemie) controlled by a personal computer. The polymer electrolyte samples (13 mm in diameter and approximately 60–100 μm thick) were put into two identical platinum blocking disk electrodes. The electrodes were held in a semi-open PTFE cell with stainless steel electrodes. A sealed glass cell with fixed platinum electrodes was used for measuring the resistance of 85% H₃PO₄. The impedance measurements were carried out from 1 Hz to 1 MHz in the temperature range 333–423 K. To confirm the stability of the ionic conductivity at low humidity and high temperature, the ionic conductivity was measured in an Ar box (the dew point is equal to −86 °C).

2.4. Fuel cell test

The membrane electrode assemblies (MEA) were prepared by stacking a couple of commercial catalyst/gas diffusion layer electrodes (0.5 mg cm^{-2} Pt loading, 30 wt.% Pt/Vulcan XC-72, E-TEK, the active areas of both the cathode and anode were 7.84 cm^2) with phosphoric acid doped PPA membranes. The Current–Voltage (IV) profile was measured using a zero volt electric load ELZ-303 (Heisoku Giken) under flowing gas (anode: H₂ 100 ml min^{-1}; cathode: air 200 ml min^{-1}) without humidification at 423 K (measurements of the gas utilizations were not attempted due to the small electrode areas). Cyclic voltammetry was performed to determine the electrochemical active surface area. An Autolabo PGSTAT30 was used for the measurements under flowing gas (anode: H₂ 100 ml min^{-1}; cathode: N₂ 200 ml min^{-1}).

3. Results

### 3.1. The proton conducting membranes

Each of the synthesized polymers had almost the same ivory white color. The molecular weights (M_w) were 376,000, 55,000 and 68,000 for PMD-Im, POD-Im and PDMDP-Im, respectively. The polymer films prepared were flexible and slightly colored transparent membranes, i.e. the color of PMD-Im and PDMDP-Im was transparent pale yellow, and POD-Im was transparent pale red. Detailed analytic data are described in Appendix A.

Each membrane changed to a deeper transparent yellow after the doping. The doping levels of the membranes after the thermal treatment and removal of the residual water are summarized in Table 1. At high H₃PO₄ concentration (e.g.

Scheme 1.

Table 1
The doping level (H₃PO₄ mol/repeat unit) of the membranes

Samples	H₃PO₄ concentration (%)			
	85	95	97	99
PMD-Im	2.4	9.4	sol[a]	sol
POD-Im	1.3	5.1	6.6	sol
PDMDP-Im	2.4	4.1	12.5	sol

[a] Soluble.
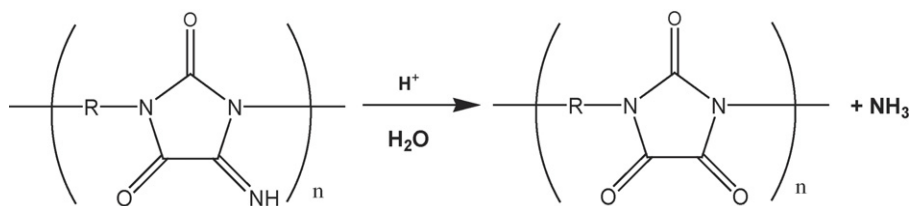
Scheme 2.

99%), the membranes dissolved to form very viscous liquids. The doping levels increased with increasing H_3PO_4 concentration in all membranes. The doping levels were the lowest in the POD-Im membranes for every phosphoric acid concentration. Different critical concentrations of dissolution were observed in concentrated phosphoric acid for the three membranes.

Since with water the "imino" group of the precursor polymers is easily converted to a "trione" in the presence of an acid (Scheme 2), FT-IR spectra were measured to observe if there was a structural change resulting from hydrolysis of the membrane electrode assembly (MEA) at high temperature.

The FT-IR spectra of the PMD-Im and the hydrolyzed PMD-Im membranes are shown in Fig. 1. It was observed that the peak at $1677 \, cm^{-1}$ for PMD-Im, which was assigned to the functional group of >C=NH, decreased with the hydrolysis. Similarly, the peaks at 1675 and $1679 \, cm^{-1}$ which correspond to >C=NH bonds decreased with the hydrolysis of POD-Im and PDMDP-Im, respectively (not shown). These results indicate that the imino group population decreased with the acid doping and the elevation of the temperature. The major parts are changed to "trione" structures. However, a small amount of imino groups still exists in the membrane as is reflected by the small residual peak. Remarkably, the doped phosphoric acid remains in the membrane after washing and only a small amount of the phosphoric acid exudes with the shrinking of the membrane resulting from the thermal treatment. After the doping, the thickness of the membranes increased two- or three-fold, however, the area of the membranes decreased by approximately 10%.
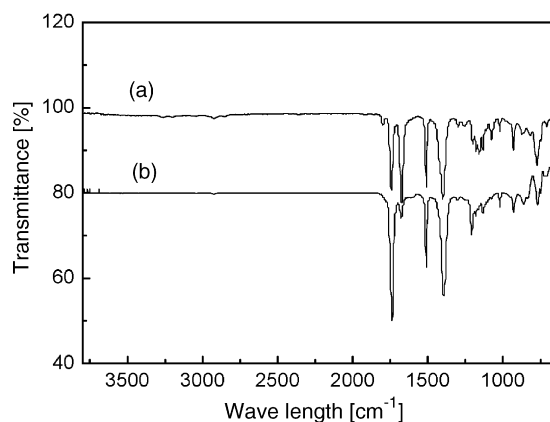
3.2. Thermal properties

The thermogravimetric curves for the three H_3PO_4 doped membranes are shown in Fig. 2. The total decomposition processes of the membranes were quite similar and three steps of weight losses were observed. The first weight loss step (∼5% reduction) appeared around 420 K due to water evaporation resulting from poly-condensation of phosphoric acid. The second step corresponded to the decomposition of polymers, and was observed around 500 K for PDMDP-Im, and 600 K for PMD-Im and POD-Im. Clearly these membranes are able to be used as ion conducting polymer electrolytes in high temperature usage since the thermal decomposition of polymers starts above 500 K.

3.3. Ionic conductivity

Arrhenius plots of the ionic conductivity (σ) for the H_3PO_4 doped membranes (and 85% H_3PO_4 as a reference) are shown in Fig. 3. The ionic conductivities of 85% H_3PO_4 doped membranes are always lower than those of the highly concentrated H_3PO_4 doped membranes. The temperature dependence of the ionic conductivity of each membrane showed an Arrhenius type behavior.

$$\sigma(T) = \sigma_0 \exp\left(\frac{-E_a}{RT}\right) \tag{1}$$

The activation energies of the ionic conductivities determined from regressing the Arrhenius equation onto the data are sum-

Fig. 1. FT-IR spectra of (a) PMDI-Im and (b) hydrolyzed PMDI-Im (after thermal treatment).
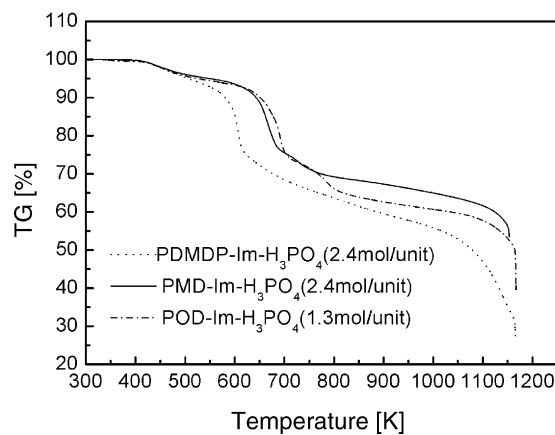

Fig. 2. TGA trace of H_3PO_4 doped (a) PMD-Im, (b) POD-Im, and PDMDP-Im. The doping levels were 2.4, 1.3 and 2.4 mol/repeat unit for PMD-Im, POD-Im and PDMDP-Im, respectively. The measurement was performed in an inert atmosphere with a heating rate of $10 \, K \, min^{-1}$.
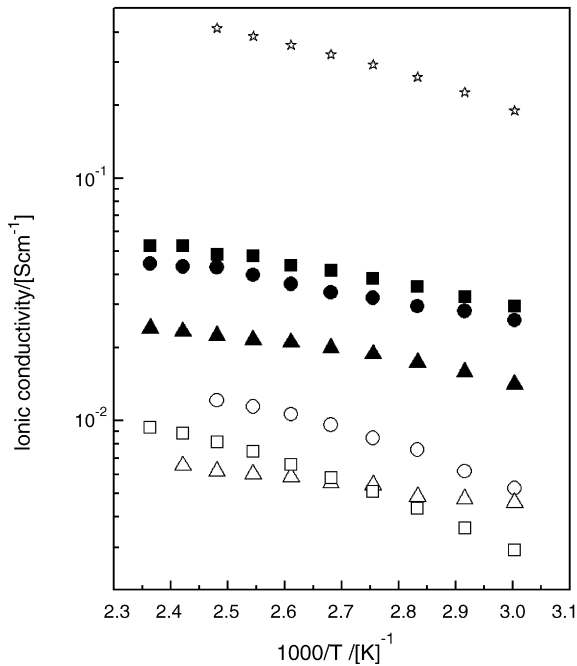
Fig. 3. An Arrhenius plot of the ionic conductivity for H_3PO_4 doped [circles: (open: 2.4 mol unit^{-1}, $t = 68$ μm) and (solid: 9.4 mol unit^{-1}, $t = 90$ μm)] PMD-Im, [triangles: (open: 1.3 mol unit^{-1}, $t = 70$ μm) and (solid: 6.6 mol unit^{-1}, $t = 145$ μm)] POD-Im, and [squares: (open: 2.4 mol unit^{-1}, $t = 69$ μm) and (solid: 12.5 mol unit^{-1}, $t = 130$ μm)] PDMDP-Im and (open star). Liquid 85% phosphoric acid was used as the reference.

marized in Table 2. The activation energy of 85% H_3PO_4 without membrane was 11.7 kJ mol^{-1} in the temperature range 343–403 K. Some of the membranes had similar E_a values, however, POD-Im and high doping level PMD-Im and PDMDP-Im gave lower activation energies.

3.4. Fuel cell demonstration

The polarization curves of the test cells using the three highly doped membranes at 423 K are shown in Fig. 4. The measurements were carried out after constant current generation at 0.3 A cm^{-2} for 100 h. The shapes of the polarization curves for each sample were similar to each other; however, PDMDP-Im had the lowest performance at limiting current at 1.0 A cm^{-2}. Although the 12.5 mol unit^{-1} H_3PO_4 doped PDMDP-Im had the highest ionic conductivity, gas cross-over might occur as a lower open circuit voltage was observed for this than in the other cells.

Table 2
Activation energies of the ionic conductivity

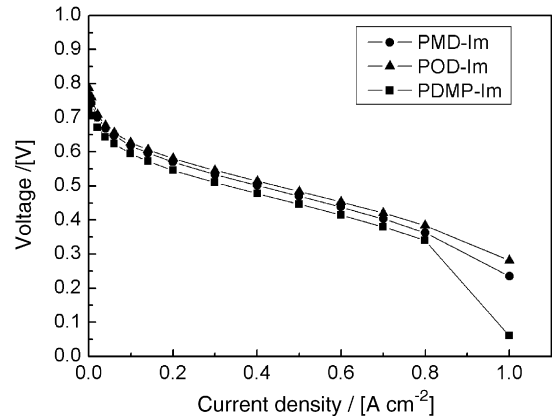| Samples	Doping level (H_3PO_4 mol/repeat unit)	E_a (kJ mol^{-1})
PMD-Im	2.4	12.7 ± 0.5
	9.4	7.4 ± 0.3
POD-Im	1.3	5.2 ± 0.7
	6.6	6.3 ± 0.6
PDMDP-Im	2.4	14.2 ± 0.6
	12.5	7.5 ± 0.3

Fig. 4. Polarization curves for test cells at 423 K without humidification. 0.5 mg cm^{-1} Pt loading, 30 wt.% Pt/Vulcan XC-72 (E-TEK GDL) was used for the cathode and anode. The flow rates of gases were H_2: 100 ml min^{-1} and air: 200 ml min^{-1}. Gas utilizations were not considered. The composition of the membranes correspond to the points on Fig. 3.

Limiting currents were observed at 1.0 A cm^{-2} for all samples, even if the gas utilizations were not attempted (enough gas was supplied for the reaction, such as $U_{fuel} = 16\%$ and $U_{air} = 20\%$ at 0.3 A cm^{-2}).

The time dependence of the closed circuit voltages in the constant current generation test of 0.3 A cm^{-2} are shown in Fig. 5. The test fuel cells were evaluated until the voltage decreased to 0.5 V. The cell open circuit voltages were 0.798, 0787 and 0.726 V for PMD-Im, POD-Im and PDMDP-Im, respectively. The poor electrochemically active surface area was presumed to be due to the absence of electrolytes in the electrodes. Cyclic voltammetry was performed to confirm the electrochemically active surface area (ECSA) for the PMD-Im cell, under flowing H_2 and N_2 gas for anode and cathode, respectively. The ECSA was determined by integration of the hydrogen adsorption peak from 0.4 to 0.05 V versus RHE, and a value of 32 cm^2 Pt mg^{-1} was obtained [11]. This value is half the ECSA of a conventional PEM electrode. A similar ECSA was presumed for the other two cells because of the similarity in the interface between GDE and the polymer membrane to that in PMD-Im. Also, linear sweep voltammetry was performed to quantify the hydrogen gas cross-over. The leak current was determined to be 1.9 mA cm^{-1}. Since
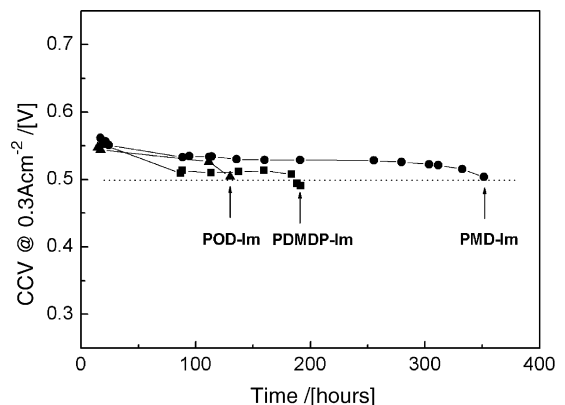

Fig. 5. Time dependence of the closed circuit voltage under constant current operation at 0.3 A cm^{-1} at 423 K without humidification.

the current was not so large, hydrogen cross-over was unlikely to be significant in the PMD-Im cell. Consequently, PMD-Im with a voltage decay rate of 165 μV h^{-1}, exhibited the best performance of the three membranes.

4. Discussion

4.1. Ionic conduction mechanism of PPAs

The H$_3$PO$_4$ doped membranes showed high ionic conductivity with low apparent activation energy in the temperature range 333–423 K. Similar activation energies were observed in the membranes, even with different doping levels. Although the ionic conductivity is governed by the H$_3$PO$_4$ concentration, the H$_3$PO$_4$ concentration does not influence the activation energy below a doping level of 1.3 mol unit^{-1} in POD-Im. These phenomena are completely different from those in H$_3$PO$_4$ doped polybenzimidazole, where the ionic conductivity and the activation energy strongly depend on the doping level [3]. In the present study, the results indicate the affinity of H$_3$PO$_4$ for the polymer framework is quite weak in the PPA membranes due to the structural change from "imino-dione" to "trione" during the hydrolysis. Actually, the completely hydrolyzed PPAs do not swell in phosphoric acid. The following hypothesis is considered in the present membranes. (1) The "imino-dione" structure has a strong interaction with H$_3$PO$_4$ bringing H$_3$PO$_4$ into the polymer matrix during the doping process. (2) The polymer structure is changed to "trione" by the hydrolysis and then some of the phosphoric acid is released. However, the micropores formed by the swelling of the membrane by H$_3$PO$_4$ is unchanged during the hydrolysis, because the polymer motion is frozen below its (high) glass transition temperature [10]. Therefore, most of the H$_3$PO$_4$ remains in the membrane, even if the population of imino groups is decreased. (3) Ammonium phosphate may be formed in the membranes, and the salt contributes to the ionic conduc-

tion. (4) Anisotropic ionic conduction is assumed in the PPA membranes, because the surface of the membrane decreased (about 10% decrease in width) and the thickness increased (about two- or three-fold) during doping. These assumptions are summarized and illustrated in Fig. 6.

4.2. Comparisons between the three membranes

PMD-Im and POD-Im are more thermally stable than PDMDP-Im. PDMDP-Im decomposes at lower temperatures due to the existence of methoxy groups in the polymer structure. Although POD-Im has an ether oxygen, the thermal decomposition is not serious in the polymer main chain below 600 K. The POD-Im test cell had the lowest performance at a constant current of 0.3 A cm^{-2}. However, this is not thought to be due to thermal decomposition. The molecular weight of each polymer is different, the effects of different polymer structures on fuel cell performance has not been clarified.

4.3. Applicability to high temperature fuel cells

Although the preliminary trials of the present membranes in the high temperature fuel cells were successful, the performances were not good enough, especially in the voltage decay rate in the constant current generation at 0.3 A cm^{-2}. The catalyst/diffusion layer was not optimized in any of the cells in this study. Clearly, the poor performance is related to the absence of proton sources in catalyst layer resulting in poor charge transfer at the three phase boundaries. A small amount of phosphoric acid can be assumed to move to the catalyst layer from the membrane due to osmosis, but the amount of phosphoric acid may not be sufficient in the electrodes. Since the thermally stable proton conducting material, phosphoric acid, was included in the membranes, the fuel cell test could be performed in a shorter time. However, a duration of 90,000 h is generally required for
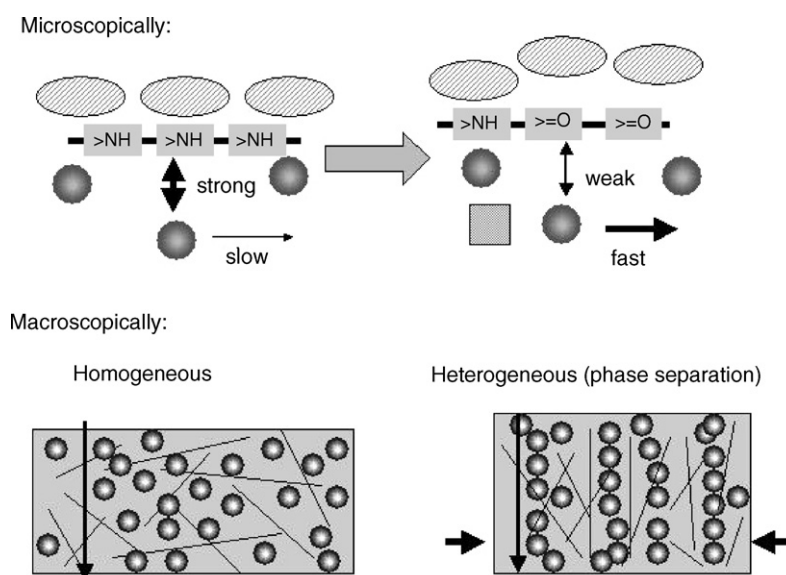

Fig. 6. An illustration of the ionic conduction models for PPAs. The interaction between polymer and ions are changed by hydrolysis. The membranes decreased in width and increased in thickness with the hydrolysis. The "trione" structure does not have an affinity for H$_3$PO$_4$.

applying to stationary fuel cells. Further improvements in the MEA fabrication process, especially in formation of a suitable three phase boundary and cell construction, are necessary for practical application in fuel cells.

5. Conclusion

Thermally stable proton conducting polymer electrolytes, H_3PO_4 doped PPA membranes exhibited high ionic conductivity with low activation energies close to that of liquid phosphoric acid. A weak interaction between the host polymer and H_3PO_4 was assumed. A fuel cell test was also performed using these membranes with constant current (0.3 A cm^{-2}) operations being attained at 423 K without humidification demonstrating the applicability of PPAs to fuel cells.

Acknowledgements

Appendix A

Analysis data for the assignments of the synthesized polymer are as follows:

- *PMD-Im*. FT-IR (KBr): 3267, 3041, 2923, 2853, 1801, 1747, 1677, 1512, 1399, 1254, 1200, 1178, 1156, 1134, 1074, 1021, 931, 773 cm^{-1}. ^{1}H NMR (400 MHz, DMSO-d_6): 4.1 (CH$_2$, 2H), 7.4–7.5 (aromatic C–H, 8H), 9.9 ppm (N–H, 1H). Elemental analysis: H 4.1, C 67.5, N 14.4, Ash 0.2% (ca. H 4.0, C 69.3, N 15.2%).
- *POD-Im*. FT-IR (ATR-Ge): 3259, 3074, 1742, 1676, 1498, 1404, 1237, 1195, 1134, 1014, 932 cm^{-1}. ^{1}H NMR (400 MHz, DMSO-d_6): 7.2–7.3 (aromatic C–H, 4H), 7.5–7.6 (aromatic C–H, 4H), 9.9 ppm (N–H, 0.8H). Elemental analysis: H 3.2, C 63.1, N 14.4% (ca. H 3.3, C 64.5, N 17.2%).
- *PDMDP-Im*. FT-IR (ATR-Ge): 2947, 2844, 1744, 1673, 1604, 1578, 1503, 1450, 1254, 1206, 1136, 1027, 841 cm^{-1}. ^{1}H NMR (400 MHz, DMSO-d_6): 4.0 (CH$_3$O, 6H), 7.5–7.6 (aromatic C–H, 6H), 10.0 (N–H, 0.5H), 10.2 ppm (N–H, 0.2H). Elemental analysis: H 4.1, C 61.4, N 12.1% (ca. H 4.1, C 63.2, N 13.0%).

References

[1] J.S. Wainright, J.T. Wang, R.F. Savinell, M.H. Litt, J. Electrochem. Soc. 142 (1995) L121–L123.

[2] J.J. Fontanella, M.C. Wintergill, J.S. Wainright, R.F. Savinell, M. Litt, Electrochem. Acta 43 (1998) 1289–1294.

[3] Y.-L. Ma, J.S. Wainright, M.H. Litt, R.F. Savinell, J. Electrochem. Soc. 151 (2004) A8–A16.

[4] P. Donoso, W. Gorecki, C. Berthier, F. Defendini, C. Poinsignon, M.B. Armand, Solid State Ionics 28 (1988) 969–974.

[5] J.C. Lassegues, B. Desbat, O. Trinquet, F. Cruege, C. Poinsignon, Solid State Ionics 35 (1989) 17–25.

[6] M.F. Daniel, B. Desbat, C. Lassegues, Solid State Ionics 28–30 (1988) 632–636.

[7] J. Grondin, D. Rodriguez, J.C. Lassegues, Solid State Ionics 77 (1995) 70–75.

[8] T.L. Patton, Polym. Preprints 12 (1971) 162–168.

[9] T. Kanbara, M. Inami, T. Yamamoto, A. Nishikata, T. Tsuru, Chem. Lett. (1990) 2263–2266.

[10] J.P. Luongo, H. Schonhorn, J. Polym. Sci. 13 (1975) 1363–1372.

[11] T.R. Ralph, G.A. Hards, J.E. Keating, S.A. Campbell, D.P. Wilkinson, M. Davis, J. St-Pierre, M.C. Johnson, J. Electrochem. Soc. 144 (1997) 3845–3857.